ABCM Symposium Series in Mechatronics - Vol. 4 - pp.179-188

AN IMPEDANCE CONTROL APPROACH FOR MACHINING TASKS USING ELASTIC JOINT MANIPULATORS

BARASUOL, V., victor@das.ufsc.br
DE PIERI, E. R., edson@das.ufsc.br
DAS - Federal University of Santa Catarina - Florianópolis/SC - CEP 88040-970

CRUZ, F. B. C., barreto@emc.ufsc.br
EMC - Federal University of Santa Catarina - Florianópolis/SC - CEP 88040-970

Abstract. *This paper presents the development of an indirect force control for robot manipulators with elastic joints employed in machining tasks. Based on the study of centralized impedance control for rigid manipulators, it is proposed an extension for robots with torsional flexibility in the joints structured as a cascade control. Additionally, it is proposed a reduced mathematical model, based on existing dynamic models of the reaction forces, that agree with the reaction forces generated by the cutting tool in contact with the environment. The present two-dimensional model relies on the tangential and normal forces on the surface, allowing to analyze the stability of the system and to obtain gain preconditions for the proposed controller, considering the parameters of the machining process. A machining task is specified for a planar manipulator with two degrees of freedom, and consists on removing the weld fillets to recover a metal surface. Simulation results for this task are presented to show the effectiveness of the proposed controller.*

Keywords: *Machining Tasks, Impedance Control, Manipulators, Flexibility.*

1. Introduction

The major obstacle that prevents the adoption of robots in processes of removing material (machining, deburring, and etc) is the fact that the stiffness of current industrial robots is much smaller than a standard CNC machine. The stiffness for an articulated robot is usually less than $1N/\mu m$, while a standard CNC machine often has stiffness greater than $50N/\mu m$. However, solutions based on CNC machinery generally present high costs, difficulting the return of invested capital.

To this end, robotics based on flexible automation appears as an ideal solution by its programmability, adaptability, flexibility, relatively low cost and especially by the results of industrial robots already employed in the foundry machinery and transport of parts in processes.

Whereas, currently, the majority of robot manipulators use harmonic drives for the transmission system, it is assumed that the major portion of flexibility is caused by these mechanisms. Therefore, since robots use indirect measurement of displacement on the drive side (motor encoders), the joint elasticity allows the individual axes to differentiate among themselves in the desired and actual positions, vibrating out of phase. This constructive arrangement has resulted in collocation problems, exhibited by a dynamic between the actuator and sensor, including non-dynamic modes in the system. This elasticity in the joints can cause an increase in the stabilization time of the manipulator and even make the system unstable (Spong, 1987).

In cases of contact tasks, is common the occurrence of non-collocated modes, since the force sensor is located on the end-effector and the motors, as the position sensors, are located before the transmission system. To face these problems in contact tasks, some impedance control strategies are presented in the literature, as Jiang et al. (2005) and Ferreti et al. (2004).

This paper, in turn, presents another impedance control strategy, which takes into account the joint elasticity to increase the task accuracy, and its stability analysis face to machining tasks.

This paper is organized as follows: first it is presented the mathematical model of the elastic joint manipulator, considered to the impedance control strategy (Sect. 2). In section 3 the impedance control strategy is developed. A simplified model of forces to the environment reactions is proposed in section 4. The stability analysis of the proposed impedance control is realized, based on the simplified model, at section 5. Finally, section 6 shows the results of simulation for a given machining task and the conclusions are presented in section 7.

2. Mathematical model of the elastic joint manipulator

Consider an open kinematic chain of n rigid links, interconnected by n joints that suffer elastic deformation. The manipulator is driven by electric actuators mounted on their joints. More precisely, consider the standard situation in which the engine i is mounted on the link $i-1$, moving the link i, and the reduction is placed before the elastic element (figure 1(b)).

For determining the equation of motion the following assumptions are made about the mechanical structure:

- The elasticity in the joints can be modeled as a spring with linear characteristics. As a torsional spring for the

ABCM Symposium Series in Mechatronics - Vol. 4 - pp.179-188

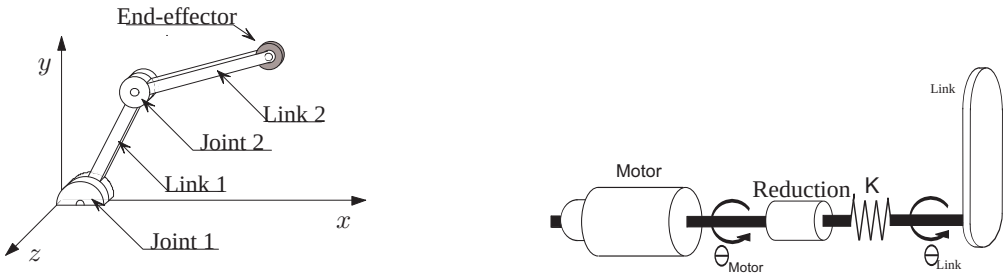

(a) (b)

Figure 1. (a) Service manipulator and (b) joint model

rotational joints and linear for the prismatic joints.

- The rotors are modeled as uniform bodies having its centers of mass on the axis of rotation.

Let q_1 be the vector $(n \times 1)$ of link positions, and q_2 the vector $(n \times 1)$ of motor positions (rotor), the mathematical model of the system can be described in joint space, based on Lagrangean Formulation, as:

$$B(q_1)\ddot{q}_1 + C(q_1, \dot{q}_1)\dot{q}_1 + g_1(q_1) = Kz \tag{1}$$

$$J\ddot{z} + B_z(q_1, \dot{q}_1, \dot{z}) + G_z(q_1, z) = u \tag{2}$$

with,

$$\begin{aligned} z &= q_2 - q_1 \\ B_z(q_1, \dot{q}_1, \dot{z}) &= -JB^{-1}(q_1)C(q_1, \dot{q}_1)\dot{q}_1 \\ G_z(q_1, z) &= JB^{-1}(q_1)[Kz - g_1(q_1)] + Kz \end{aligned} \tag{3}$$

where $B(q_1)$ is the $(n \times n)$ inertia matrix, symmetric and positive defined for all q_1, $C(q_1, \dot{q}_1)$ is the $(n \times n)$ matrix of centrifugal forces and Coriolis, $G(q_1)$ is the vector $(n \times 1)$ of gravitational forces. The rotor inertia matrix J has dimension (*n* x *n*) and is diagonal positive defined, K is the diagonal stiffness matrix $(n \times n)$ that contains the torsional constants (Readman, 1994). The subsystem (1) will be called *links subsystem* while (2) *rotors subsystem*.

Cartesian space model

Independently of the manipulator's structure, the task specifications are usually given in cartesian space, while the control actions are performed in joint space. When the function assigned to the manipulator consists in a contact tasks, it is advantageous that the control scheme is carried out in cartesian space, since the measurement of the reaction forces is obtained from this space. So, for the purpose of this paper, it is required that the mathematical model of the manipulator to be transformed to the cartesian space to obtain a suitable formulation for the control strategy. For this, we use some properties of the relational Jacobian matrix J_A:

$$\dot{x} = J_A\dot{q}_1 \rightarrow \dot{q}_1 = J_A^{-1}\dot{x} \tag{4}$$

$$\ddot{x} = J_A\ddot{q}_1 + \dot{J}_A\dot{q}_1 \rightarrow \ddot{q}_1 = J_A^{-1}\ddot{x} - J_A^{-1}\dot{J}_A\dot{q}_1 \tag{5}$$

$$u = J_A^T h_A \tag{6}$$

where h_A represents the force exerted by the manipulator in the cartesian space and the index "A", used in h_A, refers to the use of the analytical Jacobian in the mapping.

Substituting (4), (5) and (6) at (1) yields the elastic manipulator's model described in the cartesian space as:

$$\begin{aligned} \bar{B}(q_1)\ddot{x} + \bar{C}(q_1, \dot{q}_1)\dot{x} + \bar{g}(q_1) &= \bar{K}z \\ J\ddot{z} + B_z(q_1, \dot{q}_1, \dot{z}) + G_z(q_1, z) &= u \end{aligned} \tag{7}$$

where x represents the position vector of the end-effector in the cartesian space, $\bar{B}(q_1) = J_A^{-T}B(q_1)J_A^{-1}$ the inertia matrix, $\bar{C}(q_1, \dot{q}_1) = J_A^{-T}C(q_1, \dot{q}_1)J_A^{-1} - J_A^{-T}B(q_1)J_A^{-1}\dot{J}_A J_A^{-1}$ the matrix of centrifugal forces and Coriolis, $\bar{g}(q_1) = J_A^{-T}g_1(q_1)$ the matrix of gravity and $\bar{K} = J_A^{-T}K$ the stiffness matrix to the cartesian space.

ABCM Symposium Series in Mechatronics - Vol. 4 - pp.179-188

3. Impedance control for elastic joint manipulators

A parameterization in cascade of the elastic joint manipulator facilitates the synthesis of control. The strategy that will be presented below allows to obtain two blocks in closed loop whose dynamics is quasi-linear and where the equations are simpler when compared with other existing methods. This facilitates the analysis of stability and choice of parameters of synthesis, while improving the robustness of the control. This approach considers the case of strong elasticity and therefore complements the approach based on singular perturbation theory, which assumes a model where the elasticity is smaller.

The control strategy is performed in two stages. The first is to determine the desired variable z_d, which allows the linearization of the subsystem of the links and allows the injection of the control of impedance. The second is the calculation of the control torque u from z_d resulted from the first stage. The realization of this control is possible provided that the following hypotheses are met (Benallegue, 1991):

Hypothesis 2.1 - The desired trajectory for $x(t)$ is smooth and its successive time derivatives up to fourth order are continuous and limited.

Hypothesis 2.2 - The variables, x, $\dot{x}$, z and $\dot{z}$ are measurable or observable for all t.

Hypothesis 2.3 - The kinematic mapping $k_a(q_1) \rightarrow x$ is smooth and invertible, that is, the analytical jacobian is non-singular.

3.1 The impedance control in the links subsystem

Consider the dynamic equations of the links subsystem (1) under the influence of an external force:

$$\bar{B}(q_1)\ddot{x} + \bar{C}(q_1, \dot{q}_1)\dot{x} + \bar{g}(q_1) = \bar{K}(z_d - \tilde{z}) - h \tag{8}$$

where h represents an external force exerted on the end-effector and $\tilde{z} = z_d - z$.

Referring to the model (8), consider the following control law:

$$z_d = \bar{K}^{-1}[\bar{B}(q_1)u_{0x} + \bar{C}(q_1, \dot{q}_1)\dot{x} + \bar{g}(q_1)] + \bar{K}^{-1}(\bar{B}B_m^{-1} + I)h \tag{9}$$

where u_0 is an auxiliar input of control and B_m is a matrix of gains to be defined.

Substituting (9) in (8) the dynamic in the cartesian space can be described by:

$$\ddot{x} = u_0 - \bar{B}^{-1}\bar{K}\tilde{z} - h \tag{10}$$

which reveals the existence of a non-linear term coupling with the variable $\tilde{z}$.

The input control u_0 is designed to insert a desired behavior to the manipulator, that is:

$$u_0 = B_m^{-1}(B_m\ddot{x}_d + D_m\dot{\tilde{x}} + K_m\tilde{x}) \tag{11}$$

where B_m, D_m and K_m are positive defined diagonal matrices.

Substituting (11) in (10) yields the closed loop dynamic of the manipulator in the cartesian space:

$$B_m\ddot{\tilde{x}} + D_m\dot{\tilde{x}} + K_m\dot{\tilde{x}} = h + B_m\bar{B}^{-1}\bar{K}\tilde{z} \tag{12}$$

The equation (12) is second order and quasi-linear, since the right term of the equality is non-null and non-linear, and depends on the error $\tilde{z}$ of the rotors subsystem dynamics. The attributed impedance to the mechanical system is characterized by a matrix of mass B_m, a matrix of damping D_m, and a matrix of stiffness K_m. The implementation of (9) requires the feedback of the manipulator state variables $(q_1, \dot{q}_1)$ and the measurement of the contact forces h. Some considerations must be made on the controller tuning, because, even any choice for B_m, D_m and K_m, that carry physical features is possible, some complications usually appear in practice. In particular, if the position where the contact occurs is not exactly known, the diagonal elements of B_m and K_m should be chosen to avoid excessive forces of impact.

Due to disturbance $B_m\bar{B}^{-1}\bar{K}\tilde{z}$ influence in the final end-effector position, the goal of control in the second step is to make this disturbance converge to zero sufficiently fast. Having z_d designed, it remains to obtain the control law for the rotors subsystem which ensures asymptotic stability of $\tilde{z}$, corresponding to the second stage of the control strategy.

3.2 The trajectory tracking for the rotors subsystem

In the second stage the objective is to ensure the convergence rate of the error $\tilde{z}$ to zero. This convergence is achieved if performed a procedure of linearization and decoupling, both similar to that presented in the previous item. For this purpose it is calculated the control torque u for the second block as follows:

$$u = J\gamma + B_z(q_1, \dot{q}_1, \dot{z}) + G_z(q_1, z) \tag{13}$$

ABCM Symposium Series in Mechatronics - Vol. 4 - pp.179-188

where γ is an auxiliar control input that acts to obtain an error dynamic asymptotically stable in the subsystem of rotors.

Substituting (13) in (2), yields:

$$J\ddot{z} + B_z(q_1, \dot{q}_1, \dot{z}) + G_z(q_1, z) = J\gamma + B_z(q_1, \dot{q}_1, \dot{z}) + G_z(q_1, z)$$
$$J(\ddot{z} - \gamma) = 0$$

Since the matrix J is invertible:

$$J(\ddot{z} - \gamma) = 0 \quad \longrightarrow \quad \ddot{z} = \gamma \tag{14}$$

The dynamic injected by γ can now be chosen, for example, as a control PD:

$$\gamma = \ddot{z}_d + K_{D\gamma}\dot{\tilde{z}} + K_{P\gamma}\tilde{z}, \quad \tilde{z} = z_d - z \quad and \quad \dot{\tilde{z}} = \dot{z}_d - \dot{z} \tag{15}$$

where $K_{D\gamma} = K_{D\gamma}^T > 0$ and $K_{P\gamma} = K_{P\gamma}^T > 0$ are diagonal matrices of project.

Substituting (15) in (14), is obtained the following error equation in the rotors subsystem:

$$\ddot{\tilde{z}} + K_{D\gamma}\dot{\tilde{z}} + K_{P\gamma}\tilde{z} = 0 \tag{16}$$

The choice of the PD controller gains can be made seeking an error dynamic with critical damping. The dynamics of the errors in the manipulator system under the action of this control technique is generally asymptotically stable, as will be seen in section 5.

4. The machining task and the force model

Depending on the task, many parameters must be considered such as the tool tangential speed, the tool topology and grind, the direction of the tool angular velocity with respect to the feedrate direction, the workpiece stiffness, the depth of cut and the height and thickness of a burr. For example, if the material is homogeneous, then the cutting force increases proportionally to the amount of removed material. If the manipulator end-effector moves with constant speed along the contour, then the force will vary proportionally to the depth of cut. The cutting processes, however, also generate a reaction force that is not directly tangential to the surface. Indeed, the normal component of this contact force can bring problems to the control force introducing disturbances in the control loop so that the tool penetrates the workpiece or loses contact, depending on the direction of its rotation with respect to the feedrate direction.

It was observed that most authors neglect the third dimension by despise the magnitude of the contact force orthogonal to the tangential and normal vectors to the surface. The same will be done in this paper, which efforts will be considered only in normal (sub-index n) and tangential (sub-index t) directions to the surface and, consequently, a XY plan of the cartesian space that will be referenced by the sub-indices x and y.

In figures 2(a) and 2(b), can be seen the forces that act on a workpiece during the cutting process. To simplify the illustration it is assumed that every moment only one tooth of the tool is in contact with the surface and that all forces act on a single point.

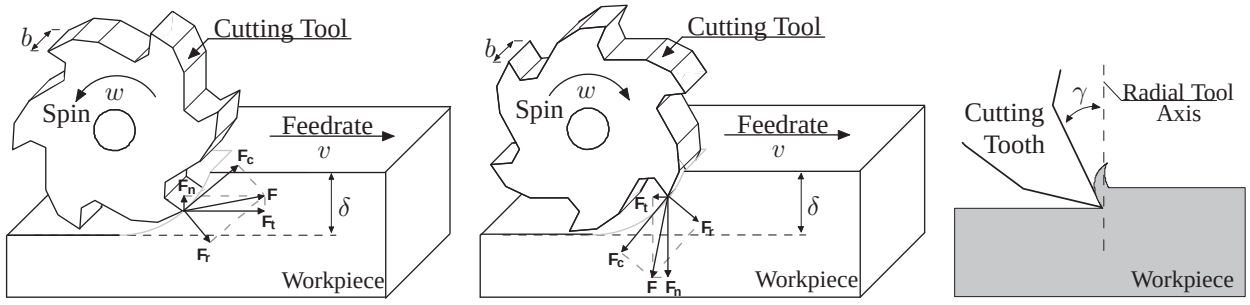

(a) (b) (c)

Figure 2.

If the tool feedrate direction coincides with the peripheral speed direction of the cutting tooth in contact with the surface (Figure 2(a)), the machining forces that act on the workpiece has a component $\vec{F}_t$ oriented as the tangential velocity, while the normal component $\vec{F}_n$ is oriented from the surface to the tool. The reaction forces generated on the tool (and measured by the force sensor) have, therefore, opposite directions to the feedrate direction characterizing a *discordant movement*. It is interesting to note that in this case the reaction normal force tends to pull the tool into the workpiece surface and it can, eventually, make the tool to penetrate overmuch and lock preventing the robot to perform the task.

ABCM Symposium Series in Mechatronics - Vol. 4 - pp.179-188

On the other side, if the tool feedrate direction is opposite to the peripheral speed direction of the cutting tooth in contact with the surface (Figure 2(b)), the reaction forces generated on the tool tend to push it from the surface while the reaction tangential force tends to increase the feedrate velocity, which features a *concordant movement*.

For each tooth of the tool in contact with the surface, there is a cutting force, $\vec{F}_c$, acting in the direction of the cutting tangential velocity and a normal force, $\vec{F}_r$, acting in the radial direction. Usually it is assumed that the radial force is proportional to the cutting force, ie,

$$F_r = F_c \, tan(\phi - \gamma) \tag{17}$$

where ϕ is the friction angle (generally difficult to estimate) and γ is the tool frontal bevel (Figure 2(c)).

The cutting force on the workpiece F_c can be expressed as (Radford, 1980):

$$F_c = \frac{b \, \delta \, v \, u}{w} \tag{18}$$

where b is the mill thickness, δ the cutting depth, v the feedrate, u is the material specific energy and w is the milling angular velocity. These parameters also present great difficulty in their estimation. In the task coordinate system, $\vec{F}_n$ and $\vec{F}_t$ represent the components of the resulting force $\vec{F}$.

Knowing that in a properly planned task of machining the cutting depth should vary proportionally with the height of the burr, the choice of the cutting depth will depend on the magnitude of the normal force that is desirable to support, which indirectly results in a proportionality between the reference to the normal force and the height of the burr. The aim of this paper is not the detailed study of the force model, however, it's necessary to define a simple and coherent representative model to perform the stability analysis. Not enough, we need to get a model that takes into account the decomposition of the normal and tangential forces in cartesian space.

Therefore, this section provides the definition of a simplified model to perform the stability analysis. A synthesis of the models found in Ziliani et al. (2007), Sugita et al. (2007), Kim et al. (2007), Pires et al. (2007), Ziliani et al. (2005), Chen and Tung (2000) and Radford (1980).

4.1 The Simplified force model

The purpose of this section is to define a simplified model of forces that explain its dependence on the main dynamic parameters: feedrate velocity and cutting depth. It is also desired that the model considers all possible directions in cartesian space to the feedrate velocity.

Then, consider initially that the cutting force, definided by equation (18), is rewritten as:

$$F_c = \frac{b \, u \, \delta \, v}{w} = f_c(\delta) v \tag{19}$$

being explicitly dependent on the cutting depth δ and feedrate velocity v, considered as time variant.

As the magnitude of this force is defined for any feedrate direction, the feedrate velocity v will be represented by the sum of its components in cartesian space $\dot{x}_x$ and $\dot{x}_y$, ie:

$$v = \dot{x}_x cos\beta + \dot{x}_y sin\beta, \quad \text{with} \quad v = \dot{x} = \frac{d}{dt} \begin{bmatrix} x_x \\ x_y \end{bmatrix} = \begin{bmatrix} \dot{x}_x \\ \dot{x}_y \end{bmatrix} \tag{20}$$

where $\beta = tg^{-1}(\dot{x}_y / \dot{x}_x)$ is the angle that relates the amplitudes of $\dot{x}_x$ and $\dot{x}_y$.

With regards to normal and tangential forces, it will be defined directly related to the cutting force through an angle α, as can be seen in figure 3:

$$\begin{aligned} F_t &= F_c \, cos(\alpha) \\ F_n &= F_c \, sen(\alpha) \end{aligned} \tag{21}$$

With these definitions it is possible to represent the cutting force in the coordinate system of the cartesian space, which is represented by $h = [F_x \; F_y]^T$, in terms of components of the feedrate velocity. Such relationships can be found in the equations (22) and (23) to the concordant and discordant movements, respectively. Figures 3(a) and 3(b) illustrate the involved vectors.

$$h = \begin{bmatrix} F_x \\ F_y \end{bmatrix} = \begin{bmatrix} -f_c(\delta) \, cos(\beta) \, cos(\alpha+\beta) & -f_c(\delta) \, sen(\beta) \, cos(\alpha+\beta) \\ -f_c(\delta) \, cos(\beta) \, sen(\alpha+\beta) & -f_c(\delta) \, sen(\beta) \, sen(\alpha+\beta) \end{bmatrix} \begin{bmatrix} \dot{x_x} \\ \dot{x_y} \end{bmatrix} = C_A^-(\delta, \beta)\dot{x} \tag{22}$$

$$h = \begin{bmatrix} F_x \\ F_y \end{bmatrix} = \begin{bmatrix} f_c(\delta) \, cos(\beta) \, cos(\alpha+\beta) & f_c(\delta) \, sen(\beta) \, cos(\alpha+\beta) \\ f_c(\delta) \, cos(\beta) \, sen(\alpha+\beta) & f_c(\delta) \, sen(\beta) \, sen(\alpha+\beta) \end{bmatrix} \begin{bmatrix} \dot{x} \\ \dot{y} \end{bmatrix} = C_A^+(\delta, \beta)\dot{x} \tag{23}$$

ABCM Symposium Series in Mechatronics - Vol. 4 - pp.179-188

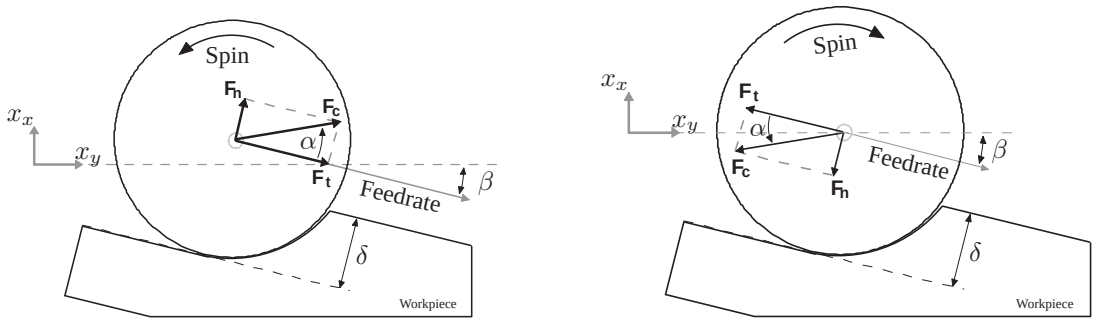

Figure 3.

For cases in which β is a multiple of $\pi/2$ the force components of the cartesian space will be the propers components of normal and tangential forces.

For the following mathematical operations are not duplicated, due to the existence of the two movements (concordant and discordant), the general notation below will be considered:

$$h = \begin{bmatrix} F_x \\ F_y \end{bmatrix} = \begin{bmatrix} C_{A11}(\delta,\beta) & C_{A12}(\delta,\beta) \\ C_{A21}(\delta,\beta) & C_{A22}(\delta,\beta) \end{bmatrix} \begin{bmatrix} \dot{x} \\ \dot{y} \end{bmatrix} = C_A(\delta,\beta)\dot{x}. \tag{24}$$

It is important to note that the matrix $C_A(\delta,\beta)$ is a limited matrix for each set of process parameters. In other words, given the machining conditions, all terms will be limited by trigonometrical functions and the cutting depth limited by the diameter of the mill. These characteristics are fundamental to the following analysis.

5. Analysis of the impedance control applied in machining task

Consider the set of equations that describe the dynamic of the elastic joint manipulator with the impedance control action:

$$B_m\ddot{\tilde{x}} + D_m\dot{\tilde{x}} + K_m\tilde{x} = h + B_m\bar{B}^{-1}\bar{K}\tilde{z} \tag{25}$$

$$\ddot{\tilde{z}} + K_D\dot{\tilde{z}} + K_P\tilde{z} = 0 \tag{26}$$

where

$$B_m = \begin{bmatrix} B_{m_x} & 0 \\ 0 & B_{m_y} \end{bmatrix}, \quad D_m = \begin{bmatrix} D_{m_x} & 0 \\ 0 & D_{m_y} \end{bmatrix} \quad \text{and} \quad K_m = \begin{bmatrix} K_{m_x} & 0 \\ 0 & K_{m_y} \end{bmatrix} \tag{27}$$

are matrices defined according the xy plan of the cartesian space. The matrices K_D and K_P remain with dimensions $(n \times n)$ while $\bar{K}$ assumes dimensions $(2 \times n)$.

Substituting the simplified force model (24), rewritten based on the velocity error $\dot{\tilde{x}} = \dot{x}_d - \dot{x}$, in (25) yields the manipulator dynamic equation for the machining task:

$$B_m\ddot{\tilde{x}} + (D_m + C_A(\delta,\beta))\dot{\tilde{x}} + K_m\tilde{x} = C_A(\delta,\beta)\dot{x}_d + B_m\bar{B}^{-1}\bar{K}\tilde{z} \tag{28}$$

$$\ddot{\tilde{z}} + K_D\dot{\tilde{z}} + K_P\tilde{z} = 0. \tag{29}$$

Rearranging these equations in a state space form, as $\dot{\rho} = A\rho + B$, where the state vector is given by $\rho = \begin{bmatrix}\dot{\tilde{x}}^T & \tilde{x}^T & \dot{\tilde{z}}^T & \tilde{z}^T\end{bmatrix}^T$, the system stability can be concluded based on the eigenvalues of the matrix A:

$$\dot{\rho} = \underbrace{\begin{bmatrix} -B_m^{-1}(D_m + C_A(\delta,\beta)) & -B_m^{-1}K_m & 0 & \bar{B}^{-1}\bar{K} \\ I & 0 & 0 & 0 \\ 0 & 0 & -K_D & -K_P \\ 0 & 0 & I & 0 \end{bmatrix}}_{Matriz\ A} \rho + \underbrace{\begin{bmatrix} B_m^{-1} \\ 0 \\ 0 \\ 0 \end{bmatrix}}_{Matriz\ B} f_{esm} \tag{30}$$

where $f_{esm} = C_A(\delta,\beta)\dot{x}_d$.

To facilitate the analysis of eigenvalues, consider the matrix A containing the following internal structure:

$$A = \left[\begin{array}{cc|cc} -B_m^{-1}(D_m + C_A(\delta,\beta)) & -B_m^{-1}K_m & 0 & \bar{B}^{-1}\bar{K} \\ I & 0 & 0 & 0 \\ \hline 0 & 0 & -K_D & -K_P \\ 0 & 0 & I & 0 \end{array}\right] = \left[\begin{array}{c|c} A_1 & A_{12} \\ \hline 0 & A_2 \end{array}\right]. \tag{31}$$

It is verified that the matrix A has 4+$2n$ eigenvalues, being 4 eigenvalues from the matrix A_1, relatives to the variables of the cartesian space, and $2n$ eigenvalues from the matrix A_2, relatives to the rotors subsystem.

The eigenvalues of the matrix A_2 are negative for any positive values of K_{Di} and K_{Pi} (relatives to the i joint) and are independent of the process parameters. These eigenvalues are described below:

$$\lambda_{1,2_i} = -\frac{K_{Di}}{2} \pm \frac{\sqrt{K_{Di}^2 - 4K_{Pi}}}{2} \qquad i = 1, 2, ..., n. \tag{32}$$

The eigenvalues of the matrix A_1 are not negatives for all values of gain and are conditioned by the parameters of the process.

To facilitate the choice of these gains, it is proposed a methodology to obtain the eigenvalues based on the resulting force orientation. Thus, at the moment that the resulting force is completely on the x_x axis, $\beta = -\alpha$ and $\beta = \pi - \alpha$, the four eigenvalues and consequently the precondition gains are given by:

$$\lambda_{5,6} = -\frac{D_{m_x} + C_{A11}(\delta,\beta)}{2B_{m_x}} \pm \frac{\sqrt{(D_{m_x} + C_{A11}(\delta,\beta))^2 - 4B_{m_x}K_{m_x}}}{2B_{m_x}} \tag{33}$$

$$\lambda_{7,8} = -\frac{D_{m_y}}{2B_{m_y}} \pm \frac{\sqrt{D_{m_y}^2 - 4B_{m_y}K_{m_y}}}{2B_{m_y}} \tag{34}$$

Likewise, for the moment that the resulting force is completely on the x_y axis, $\beta = \frac{\pi}{2} - \alpha$ and $\beta = \frac{3\pi}{2} - \alpha$:

$$\lambda_{5,6} = -\frac{D_{m_x}}{2B_{m_x}} \pm \frac{\sqrt{D_{mx}^2 - 4B_{m_x}K_{m_x}}}{2B_{m_x}} \tag{35}$$

$$\lambda_{7,8} = -\frac{D_{m_y} + C_{A22}(\delta,\beta)}{2B_{m_y}} \pm \frac{\sqrt{(D_{m_y} + C_{A22}(\delta,\beta))^2 - 4B_{m_y}K_{m_y}}}{2B_{m_y}} \tag{36}$$

Using the elements of $C_A(\delta,\beta)$ increased by $\bar{\delta}$ (the maximum cutting depth) and the equations (33) and (36), the preconditions set is obtained to choose the gains of matrices B_m, D_m and K_m that ensure the system stability:

$$\lambda_{5,6} = -\frac{D_{m_x} + C_{A11}(\bar{\delta},\beta)}{2B_{m_x}} \pm \frac{\sqrt{(D_{m_x} + C_{A11}(\bar{\delta},\beta))^2 - 4B_{m_x}K_{m_x}}}{2B_{m_x}} < 0 \tag{37}$$

$$\lambda_{7,8} = -\frac{D_{m_y} + C_{A22}(\bar{\delta},\beta)}{2B_{m_y}} \pm \frac{\sqrt{(D_{m_y} + C_{A22}(\bar{\delta},\beta))^2 - 4B_{m_y}K_{m_y}}}{2B_{m_y}} < 0 \tag{38}$$

6. Simulation results

The manipulator chosen for the simulation has only two parallel rotational joints (Figure 1(a)). This joint arrangement provides the robot two degrees of freedom that allows the execution of motion in a cartesian plane. This degree of mobility is sufficient to accomplish the simulation of the machining task, which will be detailed below, based on the force model proposed in section 4.

Due to the number of joints, the angular position vectors are composed as $q_1 = [q_{11}\ q_{12}]^T$ and $q_2 = [q_{21}\ q_{22}]^T$, where the variables q_{1i} and q_{2i} represent, respectively, the link and the rotor position related to the joint i.

The constructive parameters used in the simulation of the machining task are presented in table 1.

Table 1.

Parameter	Value	Unit	Parameter	Value	Unit
Links Length	0.25	$[m]$	Reduction	100	[-]
Link 1 Center of Mass	0.118	$[m]$	Rotors Inertia	0.00045	$[kg\,m^2]$
Link 2 Center of Mass	0.116	$[m]$	Torsional Constants	100.000	$[N/rad]$
Link 1 Mass	11.4	$[kg]$	Motors Mass	1.4	$[kg]$
Link 2 Mass	19.5	$[kg]$	Tool Mass	1	$[kg]$
Link 1 Inertia	0.23	$[kg\,m^2]$	Tool Inertia	0.1	$[kg\,m^2]$
Link 2 Inertia	0.16	$[kg\,m^2]$			

The machining task consists in the removal of strips of solder deposited on a planar surface (Figure 4(a)). For purposes of simplification, the strips of solder, projected on the robot's work plane, is approximated by a trapezoidal profile with ripples as illustrated in figure 4(b).

ABCM Symposium Series in Mechatronics - Vol. 4 - pp.179-188

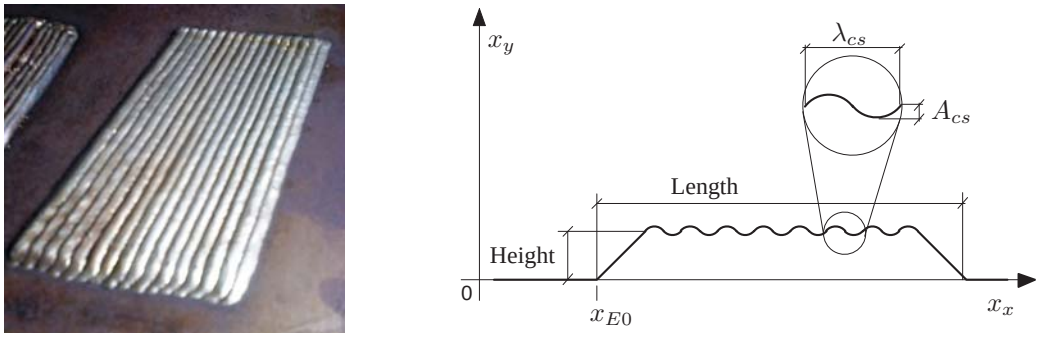

(a) (b)

Figure 4. Strips of solder profile: (a) real and (b) approximated.

Table 2.

Parameter	Value	Unit
x_{E0}	0.15	$[m]$
Length	0.25	$[m]$
Height	10.0	$[mm]$
λ_{cs}	10.0	$[mm]$
A_{cs}	3.0	$[mm]$

Table 3.

Item	Value	Unit
F_d	40.0	$[N]$
$\bar{\tilde{y}}$	1.0	$[mm]$

The values of the surface parameters chosen for the simulation are presented in table 2.

The movement performed by the manipulator consists on a single pass of concordant movement. The manipulator starts the task from the rest and without contact with the environment. It is considered in the simulation that the surface to be recovered is aligned to the x_x axis, therefore, all the acceleration and velocity references for the controller are restricted to this axis. In other words, the references of position $y_d(t)$, velocity $\dot{y}_d(t)$ and acceleration $\ddot{y}_d(t)$ for the controller are zero for all time.

It is planned that the moment of contact with the environment is occurred with the tool in a constant feedrate velocity. Arbitrarily, it is adopted a feedrate velocity of 20 mm/s for the part of contact. Instead of a trapezoidal profile to the desired velocity, it is planned a smoothed profile that avoid the presence of an unwanted motion due to non-linearities in the curve of reference, agreeing with the hypothesis of the strategy formulation.

To finish the task planning, two important items must be specified: the level of the desired force F_d under which the tool must be submitted during the pass, and the maximum material height remaining after the pass $\bar{\tilde{y}}$. These items are chosen arbitrarily, according to the table 3, and serve both to adjust the tool parameters to generate the expected forces of reaction as design the controller gains for the task.

6.1 Environment properties and tool parameters

As presented in section 4, the magnitude of the cutting force F_c, although expressed in a reduced form by the cutting depth δ and feedrate velocity v, it depends on the environment and tool features, ie,

$$F_c = \frac{b\,u\,\delta\,v}{w} = f_c(\delta)v. \tag{39}$$

The parameters related to the tool are simple to obtain, but the same can not be said with respect to the material specific energy. Because of this, to perform the simulation, the parcel bu/w is indirectly defined based on the desired feedrate velocity, denoted by v_d, and the items F_d and $\bar{\tilde{y}}$ above defined.

From the values of the maximum remaining height $\bar{\tilde{y}}$ and of the profile height, it is possible to obtain the maximum cutting depth expected:

$$\hat{\delta} = \text{profile height} - \bar{\tilde{y}} = 0.01\ m - 0.001\ m = 0.009\ m. \tag{40}$$

With the desired feedrate velocity defined as 20 mm/s and the level of the contact force as 40 N, the parcel bu/w, denoted by the coefficient c_A, can be obtained:

$$F_d = \frac{b\,u}{w}\,\hat{\delta}\,v_d = c_A\,\hat{\delta}\,v \quad \longrightarrow \quad c_A = 2.2222 \times 10^5\,\frac{Ns}{m^2}. \tag{41}$$

It is also necessary to define the angle α, shown in section 4.1 which relates the components normal and tangential of

ABCM Symposium Series in Mechatronics - Vol. 4 - pp.179-188

the cutting force. This parameter is dependent on the constructive aspects of the tool and, for the purpose of simulation, arbitrarily chosen as 30 degrees.

Finally, from the desired level of contact force and with the definition of the angle α, the magnitude of the expected force components normal and tangential for the task can be obtained as:

$$\begin{aligned} F_{td} &= F_d\, cos(\alpha) = 40\, cos(30) = 34.6\ N \\ F_{nd} &= F_d\, sen(\alpha) = 40\, sen(30) = 20.0\ N. \end{aligned} \tag{42}$$

6.2 Controller gains

To carry out the simulations is adopted a time response of 0.02 seconds for the rotors dynamic, which has proved enough to non introduce a considered disturbance in the links subsystem. The gains values obtained according the response time and adopted to the simulation are presented in table 4.

Table 4.

Gain	Value for $t_r(2\%) = 0.02\ s$
K_{D_1}	40000
K_{D_2}	40000
K_{P_1}	400
K_{P_2}	400

Table 5.

Gain	Value
B_{m_x}	10
B_{m_y}	10
D_{m_x}	2500
D_{m_y}	2500
K_{m_x}	20000
K_{m_y}	20000

The gains related to the links subsystem, B_m, D_m and K_m, are presented in table 5 and are chosen based on the preconditions obtained from the stability analysis whereas the maximum value is achieved by the elements of the matrix $C_A(\delta, \beta)$.

Simulations results for the machining task are presented in figures 5, 6 and 7 for an ideal case of implementation. In this situation is considered that all the state variables needed to close the loop control are available by full instrumentation. In the figures is shown the robot performance for two cases: one consists on the use of an impedance control strategy based on the robot rigid model (I.C.R.M.) to control an elastic joint robot, and the other one is the proposed strategy that considers the joints elasticity (I.C.).

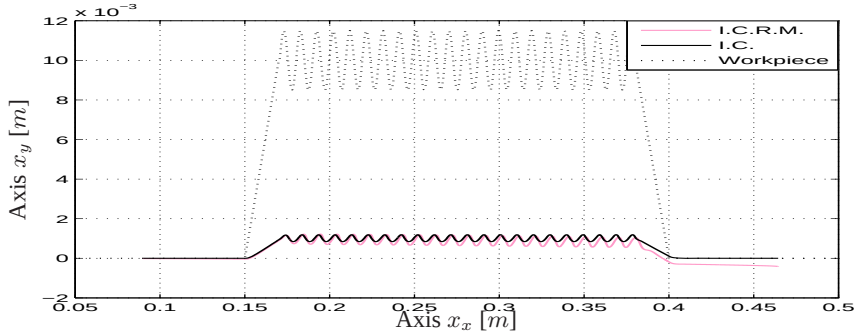

Figure 5.

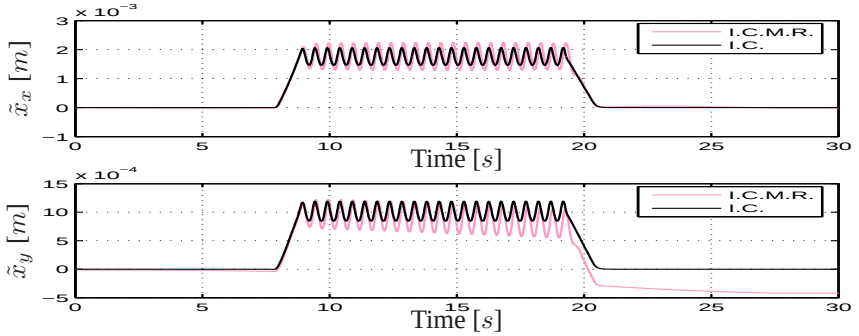

Figure 6.

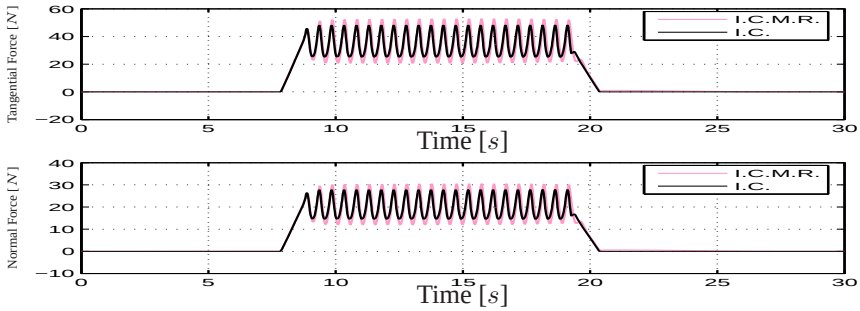

Figure 7.

Note that, despite ripples due to strips of solder, the system presents smooth responses to variations on the surface and all the predetermined criteria are met. The static positioning error caused by elasticity in the joints, that increases directly with the distance between the end-effector and its base, is compensated and considerably reduced. The results also present a reduction in the amplitude of the oscillations caused by the strips of solder.

Since the controller strategy compensates the elastic effects, the system performance is strongly affected by imprecisions in the elastic constant K. Actually, this parameter is not constant and varies with respect to the payload, as seen, per example, in harmonic drive manuals. This complementary analysis can be found in Barasuol (2008), where is shown that, with imprecisions of $\pm 10\%$ in the elastic constant, the system remains stable although it presents positioning errors.

7. Conclusion

The results obtained by simulation shows the effectiveness of the cascade design for elastic joint manipulators and verify the methodology used to choose the controller gains, held on the preconditions obtained by the stability analysis of the system. By using the proposed simplified force model for stability analysis, it was observed that the system stability is related to the D_m gain. This conclusion makes such gain the primordial adjust for the impedance controller to ensure a security task.

8. References

Barasuol, V. (2008). Controle de Força Indireto para Manipuladores com Transmissões Flexíveis Empregados em Tarefas de Esmerilhamento. Master Thesis, Federal University of Santa Catarina.

Benallegue, M. (1991). Contribution à la Commande Dynamique Adaptative des Robots Manipulateurs Rapides. Doctoral Thesis, Universite Paris, France.

Chen, S.-C. and Tung, P.-C. (2000). Trajectory planning for automated robotic deburring on an unknown geometry. Int J Mach Tools Manuf, Vol. pp. 957-78.

Ferretti, G., Magnani, G. A. and Rocco, P., "Impedance control for elastic joint industrial manipulators", IEEE Transactions of Robotics and Automation, vol. 20, no. 3, pp. 488-498, 2004.

Jiang, Z.-H., "Impedance control of flexible robot arms with parametric uncertainties", Journal of Intelligent and Robotic Systems, vol. 42, pp. 113-133, 2005.

Kim, C., Chung, J. H., and Hong, D. (2007). Coordination control of an active pneumatic deburring tool. Robotics and Computer-Integrated Manufacturing, Vol. pp. 462-471.

Pires, F. N. and Afonso, G. (2007). Force control experiments for industrial applications: a test case using an industrial deburring example. Assembly Automation, Vol. 27, No. 2, pp. 148-156.

Radford, J. (1980). Production engineering technology. McMillan Press.

Readman, M. C. (1994). Flexible Joint Robots. Mechatronics. CRC Press.

Spong, M. W. (1987). Modeling and control of elastic joint robots. J. of Dynamic Systems, Measurements, and Control, Vol. 109, No. 4, pp. 310-319.

Sugita, S., Itaya, I., and Takeuchi, Y. (2004). Development of robot teaching support devices to automate deburring and finishing works in casting. Int J Adv Manuf Technol, Vol. pp. 183-9.

Ziliani, G., Visioli, A., and Legnani, G. (2005). A mechatronic design for robotic deburring. IEEE ISIE 2005, Vol. pp. 1575-1580.

Ziliani, G., Visioli, A., and Legnani, G. (2007). A mechatronic approach for robotic deburring. Mechatronics, Vol. pp. 432-441.

9. Responsibility notice

The author(s) is (are) the only responsible for the printed material included in this paper.